ENVIRONMENTAL RESEARCH
LETTERS

LETTER • OPEN ACCESS

Measuring tropical rainforest resilience under non-Gaussian disturbances

To cite this article: Vitus Benson *et al* 2024 *Environ. Res. Lett.* **19** 024029

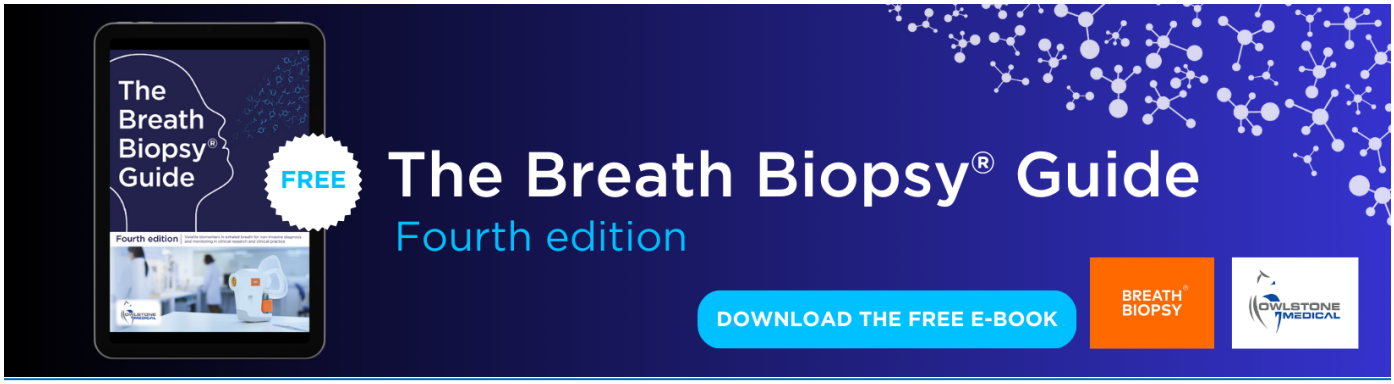

ENVIRONMENTAL RESEARCH
LETTERS

LETTER

Measuring tropical rainforest resilience under non-Gaussian disturbances

Vitus Benson[1,2,3,*], **Jonathan F Donges**[2,4,5], **Niklas Boers**[6,7,8], **Marina Hirota**[9,10], **Andreas Morr**[6,7], **Arie Staal**[4,11], **Jürgen Vollmer**[3] and **Nico Wunderling**[2,4,5,*]

[1] Biogeochemical Integration, Max Planck Institute for Biogeochemistry, 07745 Jena, Germany
[2] Earth System Analysis, Potsdam Institute for Climate Impact Research (PIK), Member of the Leibniz Association, 14473 Potsdam, Germany
[3] Institute for Theoretical Physics, University of Leipzig, 04103 Leipzig, Germany
[4] Stockholm Resilience Centre, Stockholm University, Stockholm, SE-10691, Sweden
[5] High Meadows Environmental Institute, Princeton University, Princeton, NJ 08544, United States of America
[6] Earth System Modelling, School of Engineering and Design, Technical University of Munich, Munich, Germany
[7] Complexity Science, Potsdam Institute for Climate Impact Research (PIK), Member of the Leibniz Association, 14473 Potsdam, Germany
[8] Department of Mathematics and Global Systems Institute, University of Exeter, Exeter, United Kingdom
[9] Department of Physics, Federal University of Santa Catarina, Florianopolis, 88040-900-SC, Brazil
[10] Department of Plant Biology, University of Campinas, Campinas, 13083-970-SP, Brazil
[11] Copernicus Institute of Sustainable Development, Utrecht University, Utrecht 3584, CB, The Netherlands
[*] Authors to whom any correspondence should be addressed.

E-mail: vbenson@bgc-jena.mpg.de and nico.wunderling@pik-potsdam.de

Keywords: resilience, tropical rainforest, critical slowing down, levy noise, tipping behavior, Amazon, forest disturbance

OPEN ACCESS

RECEIVED
13 October 2023

REVISED
8 January 2024

ACCEPTED FOR PUBLICATION
15 January 2024

PUBLISHED
26 January 2024

Abstract

The Amazon rainforest is considered one of the Earth's tipping elements and may lose stability under ongoing climate change. Recently a decrease in tropical rainforest resilience has been identified globally from remotely sensed vegetation data. However, the underlying theory assumes a Gaussian distribution of forest disturbances, which is different from most observed forest stressors such as fires, deforestation, or windthrow. Those stressors often occur in power-law-like distributions and can be approximated by α-stable Lévy noise. Here, we show that classical critical slowing down (CSD) indicators to measure changes in forest resilience are robust under such power-law disturbances. To assess the robustness of CSD indicators, we simulate pulse-like perturbations in an adapted and conceptual model of a tropical rainforest. We find few missed early warnings and few false alarms are achievable simultaneously if the following steps are carried out carefully: first, the model must be known to resolve the timescales of the perturbation. Second, perturbations need to be filtered according to their absolute temporal autocorrelation. Third, CSD has to be assessed using the non-parametric Kendall-τ slope. These prerequisites allow for an increase in the sensitivity of early warning signals. Hence, our findings imply improved reliability of the interpretation of empirically estimated rainforest resilience through CSD indicators.

1. Introduction

The Amazon rainforest is considered a crucial component of the Earth's climate system [1] and has been suggested as an Earth system tipping element [2–4]. There is growing concern that various anthropogenic stressors, such as climate change and associated changes in rainfall patterns, fires, land-use change and deforestation, cause a decrease in resilience and could ultimately lead to large-scale shifts in the Amazon ecosystem, with severe consequences for the biosphere and human societies [5–8]. Based on conceptual models and observational data, it is believed that the rainforests exhibits the potential for multi-stability at specific levels of moisture supply [9–13]. This means that certain regions of the rainforests may transition from a rainforest to a savanna-like vegetation state if local precipitation rates are decreased below critical thresholds.

Tropical rainforests, such as the Amazon basin, are subject to multiple stressors [14, 15]. These can originate due to weather (e.g. droughts, heat waves, windthrows), hydrology (e.g. landslides and water table dynamics), biotic factors (e.g. insect outbreaks) or anthropogenic activity (e.g. deforestation, wildfires). Such stressors cause disturbance events, which in turn change the forests in a pulse-like manner. The consequences of disturbances are often visible in the canopy gap structure, i.e. single disturbance events destroy entire parts of the forest, while neighboring parts are almost completely undisturbed. This gap structure has been observed to follow power-law-like distributions [16–24]. In other words, there is a scale-free nature to the gaps, and very large gaps are likely. These power-law-like distributions have also been observed directly for droughts [25], carbon cycle extremes [26, 27] and wildfires [28, 29] in different ecoregions worldwide. Hence, if we understand disturbances as random perturbations to the forest, i.e. as noise, this noise might have non-Gaussian characteristics. For instance, the noise could be heavy-tailed (e.g. power-law tails). Thus, extreme events become more likely than under Gaussian white noise. Furthermore, Gaussian noise would lead to continuous forest state evolutions, whereas noise due to disturbance events would result in discrete jumps in the time series. Of course, describing all disturbances by one abstract probability distribution is a highly reductive approach given the complexity of the system, yet if it were to be done, a non-Gaussian distribution should not be ruled out.

The resilience of tropical rainforests is usually measured as the response to disturbances directly from observed time series data. The recovery rate to disturbances is related to the temporal autocorrelation of a time series. If a forest is resilient and quickly recovers, the autocorrelation is lower compared to a higher autocorrelation of a more vulnerable forest that slowly recovers. Increased autocorrelation in tropical rainforests worldwide has been found using different remotely-sensed vegetation proxies such as above-ground biomass (accounting for water stress, deforestation and vapor-pressure deficit, [14]), vegetation optical-depth ([7] only Amazon basin, and [30] globally), normalized difference vegetation index (NDVI) [31] and kernel NDVI [32].

Interpreting the autocorrelation as an indicator of resilience requires certain mathematical assumptions [33, 34], under which the autocorrelation can also serve as an early warning signal in the approach to a critical transition [35]. The underlying phenomenon, called critical slowing down (CSD), traces a decreasing ability of a system to recover from perturbations when it loses stability. Typically, Gaussian noise is assumed. This is because an analytical relationship between the classical CSD indicators, named variance and temporal autocorrelation of lag one, and the recovery rate λ of the dynamics linearized around a given equilibrium can be established [36, 37] (see below). However, because it is not clear that the disturbances occurring in tropical rainforests can be described with Gaussian noise, it is doubtful whether forest resilience can effectively be measured via autocorrelation metrics.

In this paper, we study forest resilience indicators for the non-Gaussian noise case. There are various possible noise distributions to this purpose. Here, we focus on α-stable Lévy noise, for three reasons: (1) it is a heavy-tailed generalization of the Gaussian distribution, with tails that follow a power-law (i.e. extreme events become more likely). (2) The noise time series contains jumps, which is in line with discrete disturbances events that happen as abrupt burst-like pulses (e.g. wild fires or wind throws). (3) The α-stable distributions are the limit distributions for sums of random variables with infinite variance [38–40], i.e. they encompass different heavy-tailed phenomena. These characteristics serve well in representing the ones we postulate for disturbances in tropical rainforests in different temporal scales [41]. Hence, it is necessary to understand whether the CSD-based resilience indicators still perform well for Lévy noise. Additionally, we look at pink noise, which contains power-law tails, but no jumps. Previous work has already looked at red noise and time-correlated noise [36, 37, 42]. Of course, our approach of employing 1D non-Gaussian noise distributions is reductive, as it can not represent all possible temporal and spatial patterns [43, 44]. Yet, since the presence of non-Gaussian noise is plausible for tropical rainforests, the correct functioning of resilience indicators and early warning signals before critical transitions should be assessed thoroughly.

For this assessment, we use a simple conceptual tipping element model of a tropical rainforest system [45]. This model can represent a real tropical rainforest at the highest level of abstraction, capturing only the stabilising and destabilising feedbacks of the spatially extended system. It gives a reasonable first-order approximation to the tipping structure [45, 46], i.e. the bi-stability of tropical ecosystems which could either be a rainforest or a savannah state [9]. For our analysis of forest resilience, it therefore constitutes a good starting point. The argument is a similar one as before: if the indicators do not work in such a simple setting, it is unlikely they would work if real rainforests were to be observed or modelled in more detail.

2. Methods

Conceptual model of a tropical vegetation ecosystem for simulating regime shifts. In this work, we investigate tropical rainforest resilience under power-law noise. Forest resilience is frequently measured with indicators exploiting CSD, such as

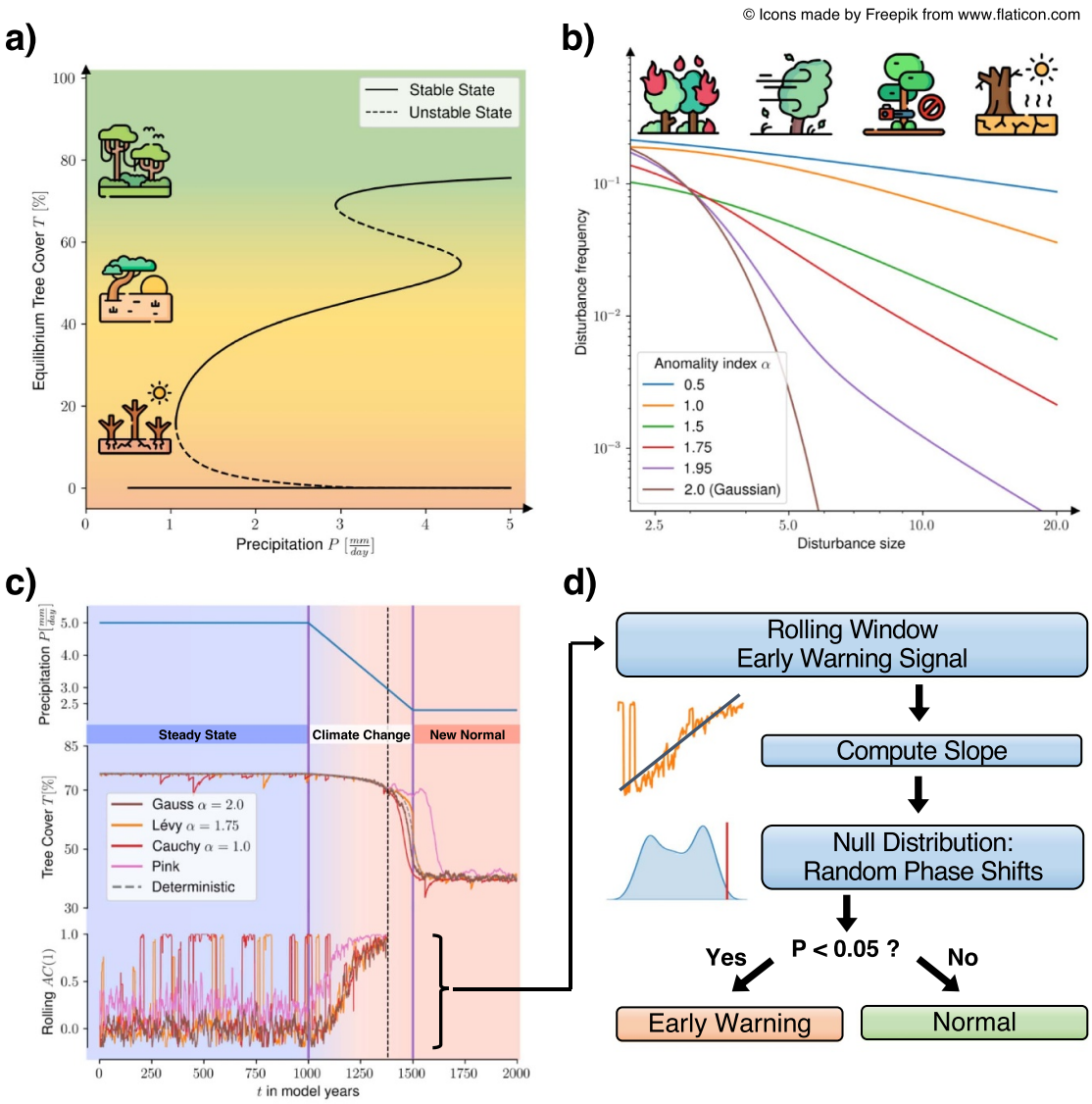

Figure 1. Overview of the study design. (a) Tropical rainforest model bifurcation diagram: depending on the precipitation level, three different equilibrium states may exist, namely rainforest, savannah and desert. © Icons made by Freepik from www.flaticon.com. (b) Many natural stressors can be modeled through α-stable Lévy noise, i.e. in contrast to Gaussian noise ($\alpha = 2$), the tails have power-law decay and hence large events can happen. © Icons made by Freepik from www.flaticon.com. (c) We simulate a climate change scenario, during which we force the precipitation level to decrease below the critical threshold of the rainforest-savannah transition. We compute the rolling autocorrelation $AC(1)$ before the critical transition and observe increases near single large disturbance events and in approach to the critical transition. (d) The CSD indicator time series (in this case: $AC(1)$) gets converted into a binary early warning indicator. For this, first a slope is calculated in a window approaching the critical transition. Then, the statistical significance of this slope is assessed by comparing to a null distribution of random phase shift surrogates with a one-sided test. If the slope is significant, there is early warning (i.e. decreasing rainforest resilience).

the autocorrelation. The phenomenon describes a decreased stability of a system up to the point where the system undergoes a critical transition and switches into another state. Hence, the estimation of forest resilience is typically an identical process as the study of early warning to critical transition, such as early warning of tipping elements in the Earth system.

In order to test the reliability of early warning signals (forest resilience indicators), we simulate rainforest-savannah transitions of a tropical rainforest using the conceptual model by van Nes *et al* [45]. Thus, our theoretical approach provides evidence necessary to understand actual measurements that may be influenced by non-Gaussian noise.

In this model, the tree cover T [%] of the rainforest is a tri-stable system with forest, savannah and treeless states depending on the precipitation P ($\mathrm{mm\,d^{-1}}$) as an external forcing. Ignoring the treeless state, the model dynamics locally exhibit the following characteristics: for $2\,\mathrm{mm\,d^{-1}} < P < 2.94\,\mathrm{mm\,d^{-1}}$ only a stable savannah state exists, for $2.95\,\mathrm{mm\,d^{-1}} < P < 4.41\,\mathrm{mm\,d^{-1}}$ both a stable savannah and a stable forest state exist and for $4.42\,\mathrm{mm\,d^{-1}} < P < 5\,\mathrm{mm\,d^{-1}}$ only a stable forest state exists (figure 1(a)). These regimes result from a governing equation [45], which without displaying units reads

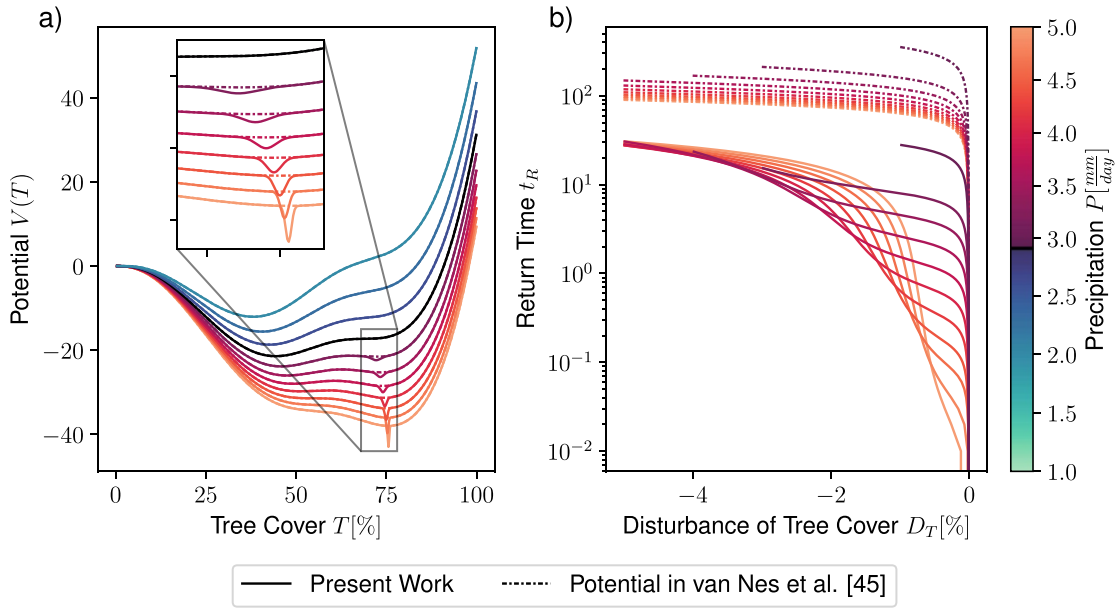

Figure 2. (a) The potential landscape of the tropical vegetation model used in this study, for varying precipitation levels (colors). The dotted line represents the original potential used in [45]. The solid line includes the modifications to represent short timescales introduced in this work. The black lines indicate the potential at $P = 2.943\,\mathrm{mm\,d^{-1}}$, which is the tipping point for the rainforest model, higher precipitation values (in red colors) allow for a stable rainforest state, while for lower precipitation values (in blue colors) only a stable savannah state exists. (b) The return time it takes for the forest to recover from a disturbance. In the original van Nes *et al* [45] model (dash-dotted), return times even for very small disturbances are in the hundreds of years. Our work adds short timescales (solid), i.e. recovery from small disturbances e.g. due to synoptic-scale weather variations is quick.

$$\frac{\mathrm{d}T}{\mathrm{d}t} = \frac{0.3P}{0.5+P}T\left(1-\frac{T}{90}\right) - \frac{1.5T}{T+10} - \frac{0.11\cdot T}{\left(\frac{T}{64}\right)^7+1}. \tag{1}$$

Here, the first term describes a logistic growth of tree cover with a precipitation-dependent expansion coefficient. The second term accounts for the Allee effect: if the tree cover is low, new trees have a harder time growing because they have less protective covering from older trees. The third term introduces a wildfire effect: dense forests are subject to higher fire mortality. While this model represents a strongly stylised way to model the dynamics of tropical vegetation, its simplicity is central to our study as it allows for many simulations of critical transitions.

Model modification to include forest response on short timescales. Originally, the van Nes *et al* [45] tipping model was developed to model critical transitions on long timescales. To investigate early warning for such critical transitions, a system response on short timescales is necessary because all CSD indicators are based on an increasing disturbance recovery time as a tipping point is approached. In the original van Nes *et al* [45] rainforest model, recovery from even very small disturbances would take hundreds of years (figure 2(b), dashed lines). This can be loosely understood as the removal of a few trees and subsequent regrowth. However, small changes in the rainforest state T could also be understood as a response to climate variations, i.e. small fluctuations due to weather systems. For instance, during a drier than usual period, trees might develop fewer leaves, but already a couple of months later they could completely recover (compare [47–50]). Recent work [51, 52] has shown a slow response of Amazonian rainforest to dry season intensification in terms of forest species composition, indicating a fast recovery from disturbances is possible. Furthermore, it is reasonable to assume faster recovery in cases of relatively small forest openings due to pulse-like disturbances like wind throw and small fires. In such cases, the surrounding remaining stands may help with faster recruitment and subsequent canopy closure. However, there are also cases of slow forest response: for long-term climatic changes (e.g. in precipitation or temperature) field evidence has been presented indicating slower mortality [53–55], with similar processes potentially also causing slower recovery. Note that the forest response to weather systems can be highly nonlinear, as trees have several regulating mechanisms (e.g. stomatal control or hydraulic resistance), which may render the forest fairly stable even under stronger climatic fluctuations. Still, it is reasonable to argue that there is the possibility for the mature rainforest to quickly recover from small perturbations which may loosely be understood as synoptic variations.

We introduce this net response to small fluctuations into the model by adding an additional short-term resilience term to equation (1). This leads to

the following changes in the potential: around the stable fixed point, we create an additional potential valley, decreasing in depth as the rainforest-savannah tipping point is approached. Figure 2(a) displays the changes: a little peak parametrized by a Gaussian exponential function centred at the rainforest attractor (right-most minimum of the potential) is subtracted from the original potential (figure 2(a), dashed lines). This additional stabilizing force strongly reduces the return times from small disturbances (figure 2(b), solid lines). The updated model equations, again displayed without units, are:

$$\frac{\mathrm{d}T}{\mathrm{d}t} = \frac{0.3P}{0.5+P}T\left(1-\frac{T}{90}\right) - \frac{1.5T}{T+10} - \frac{0.11\cdot T}{\left(\frac{T}{64}\right)^7+1} \tag{2}$$

$$-\left(\tanh\left(25P-75\right)+1\right)\frac{5}{2}\frac{\Delta T_{\mathrm{fix}}\left(T,P\right)}{\exp\left(5-P\right)^3} \times \exp\left(-\frac{5}{2}\frac{\Delta T_{\mathrm{fix}}\left(T,P\right)^2}{\exp\left(5-P\right)^2}\right) \tag{3}$$

$$+\,\mathrm{d}N_t. \tag{4}$$

Here, $\Delta T_{fix}(T,P) = T - T_{\mathrm{fix}}(P)$ is the distance to the rainforest fixed point at given P. We chose the height and width of the Gaussian such that the return time of a 1% tree cover disturbance at $P = 5\,\mathrm{mm\,d^{-1}}$ is approximately one month. The width is decreased exponentially ($\exp(5-P)$) with lower P and the height is decreased by a scaled sigmoid ($\tanh(25P-75)+1$) such that close to the savannah transition it vanishes. In addition, the new term $\mathrm{d}N_t$ represents noise increments.

Simulating rainforest disturbances with α-stable Lévy noise Multiple stressors influence tropical rainforests. Many of these occur as single, discrete, events. For instance, wildfires or windthrows may destroy parts of the forest within a few hours. The outcome is subsequently visible in the canopy gap structure. Commonly, the observed fragmentation patterns of tropical rainforests, in particular the Amazon, follows a power-law-like distribution [16–24, 56, 57]. This means, patches of all sizes exist, and particularly large gaps are observed more frequently than they would be if their origin was a random Gaussian noise process. In reality, the disturbance distribution alone does not cause the observed gap structure. Instead, complex spatial and temporal mechanisms are at play. However, as droughts [25] and wildfires [29] can also follow power-law-like distributions, it is possible that random perturbations in tropical rainforests follow a non-Gaussian distribution, possibly with power-law tails.

In this work, we assess via simulations whether CSD can be detected if the underlying noise distribution is not Gaussian but has power-law tails with jumps. For random variables with power-law tails (and thus infinite variance), a generalized central limit theorem holds [38, in section 35 theorem 5]. The limit distributions belong to the family of α-stable Lévy noise [58]. This is a family of distributions with parameters $\alpha \in (0,2], \beta \in [-1,1]$ that generalizes the Gaussian distribution (containing it at $\alpha = 2, \beta = 0$). We choose $\beta = -1$, to simulate negative disturbances, the resulting tail behaviour in a log-log plot is shown in figure 1(b). For $\alpha < 2$, the tails follow a power-law [59, 60]. In this work, we use α-stable Lévy noise $L^\alpha(\sigma;\beta)$ with amplitude σ as noise increments in our models:

$$\mathrm{d}N_t \sim L^\alpha\left(\mathrm{d}t^{\frac{1}{\alpha}}\sigma;\beta=-1\right). \tag{5}$$

Such Lévy noise leads to jumps in the forest trajectory if $\alpha < 1$, which could represent single, rapid events such as wildfires [29] or windthrows [57].

Early warning of regime shift with CSD indicators When a system approaches a tipping point, CSD measures the gradually declining recovery rate of the linearized dynamics and can be used as an early warning indicator [35, 61–63]. Here, CSD refers to an increase in the recovery time from perturbations as the system approaches a bifurcation. Measured by the rate of recovery from small perturbations, the phenomenon is used to assess ecological resilience and to warn before a critical transition is reached. The theoretical justification for using the standard deviation and the autocorrelation as CSD indicators arises from first linearizing the dynamics around a given stable fixed point x^* to obtain the linear Langevin equation

$$\mathrm{d}x = \lambda\left(x-x^*\right)\mathrm{d}t + \sigma\mathrm{d}B_t \tag{6}$$

where B_t is a Wiener process. The solution is an Ornstein–Uhlenbeck process, for which analytic expressions of both classical CSD indicators can be derived [64]:

$$\mathrm{Var}\left[x\right] = -\frac{\sigma^2}{2\lambda} \tag{7}$$

$$\mathrm{AC1}\left[x\right] = \exp\left(\lambda\Delta t\right), \tag{8}$$

where $\Delta t > 0$ is the sampling time step. Clearly, in approach to a critical point at which the linear restoring rate vanishes ($\lambda \nearrow 0$), both indicators increase monotonically ($\mathrm{Var}[x] \nearrow \infty$, $\mathrm{AC1}[x] \nearrow 1$). This statement holds also for equation (2) with a more general Gaussian noise term $\mathrm{d}N_t$. However, if the noise term follows an α-stable Lévy distribution with $\alpha < 2$, variance and AC(1) are ill-defined because the second moment of x would be infinite. Since the EWS assessments inherent to this study are always performed on a bounded state space, this poses no practical problem and an analogous CSD characteristic to that seen for the Gaussian white noise case can indeed be analytically motivated (see appendix C for further discussion). We will assess the numerical behaviour of the above indicators using simulations

with disturbances that follow such power-law noise with jumps. Furthermore, we assess the performance of the interquartile range (IQR), an indicator of the width of a distribution similar to the standard deviation, yet more robust to outliers. Even though we do not give exact analytical expressions for the IQR, CSD suggests that as a critical point is approached, the IQR increases monotonically (IQR $\nearrow \infty$).

The concrete protocol follows Boers [64] and is depicted in figures 1(c) and (d). We simulate 1000 model years of steady state, followed by 500 years of climate change and 500 years in a new steady state. During the simulated climate change, the forcing parameter precipitation is changed from 5.0 mm d^{-1} to 2.5 mm d^{-1}. Hence, the forest undergoes a critical transition with the rainforest state ceasing to exist around 1400 years at a value of 2.943 mm d^{-1}. We simulate realizations of systems under such forcing with sampled noise. To study the actual noise independent of the underlying drift, we subtract a deterministic trajectory from each stochastic realization. Note that this optimal way of nonlinearly detrending the time series—a necessary processing step prior to computing CSD indicators—is only possible in model systems. When working with observational data, one has to rely on suitable low-pass filtering. We then compute moving-window early warning signals with a window size of 10 model years. From these indicators, we compute a slope. We assess if the slope is increasing by comparing it with a null distribution of slopes of the same time series perturbed under random phase shifts. If the ground truth time series were strictly monotonically increasing, then all surrogate time series would have a lower slope (as there is no other ordering that would preserve the monotonicity). For our purpose, we set a one-sided significance level of 5%. Hence, if the observed slope lies among the 5% highest slopes of the surrogate null distribution, then it is deemed significant and hence early warning is confirmed.

3. Results

Early warning with few misses and few false alarms is possible under Lévy noise according to our experiments. We quantify the rate of achieving accurate early warnings with the recall, the fraction of correctly predicted transitions (true positives, *TP*) over all transitions (true positives and false negatives, *FN*). In other terms, the recall is high if no critical transition is missed, and low, if there are too few early warnings.

$$\text{Recall} = \frac{TP}{TP + FN}. \tag{9}$$

To study false alarms, we assess our early warning classification pipeline over random 50 year windows of the simulated steady-state years (which have no critical transition). We quantify the rate of false alarms with the false positive rate (FPR), i.e. the fraction of transitions predicted (false positives, *FP*) over all assessed transition-free time windows (false positives and true negatives, *TN*). In other terms, the FPR is low if there are no false alarms, and high, if there are too many early warnings.

$$\text{FPR} = \frac{FP}{FP + TN}. \tag{10}$$

When resolving small timescales and assessing CSD with the non-parametric Kendall-τ slope, we find an high average recall of 0.99 (figure 3(c)). Hence, early warning works with few misses. This corresponds to a measure of forest resilience that is able to detect destabilization, i.e. a decline in the system's resilience. More specifically, the early warning pipeline displays a high recall (on average 0.99) across all combinations of noise amplitude σ and Lévy index α that can be considered as weak noise levels. This suggests that within the employed limits both parameters do not strongly affect the performance of the CSD indicators. The depicted early warning pipeline entails the usage of the IQR as an early warning indicator and the Kendall-τ to assess an increasing slope. In addition, the underlying time series data was generated by our model modification which resolves short timescales.

In cases that small timescales are not resolved, we obtain a low average recall of 0.11 (figures 3(b) and (d)). Moreover, the recall is low across all admissible parameter combinations. Notably, also for Gaussian noise ($\alpha = 2$), the early warning does not work. This is due to the relatively long recovery time scale ($\mathcal{O}(100)$ model years) for even small perturbations of a few percent in tree cover (figure 2(b), dash-dotted lines) being on the same order of magnitude as the simulated critical transition ($\sim$500 model years climate change, figure 1(c). Hence, the Van Nes model is in a transient state with regards to the simulated perturbations, which inhibits the applicability of CSD indicators. In other terms, if this were the case for the real world, i.e. the rainforest would only respond very slowly to perturbations, a declining forest resilience would not be measurable with CSD indicators. Note, this result does not discredit the van Nes *et al* [45] model in general, rather it just renders it unsuitable for testing CSD indicators on noise timescales of months to years. Thus, this result justifies why in this work we extend the original model with a conceptual modification to account for short timescales, thereby making it more realistic and suitable for testing CSD indicators. Hence, in the following, we will only consider modelled time series including this modification, in which a response to disturbances on short timescales is resolved.

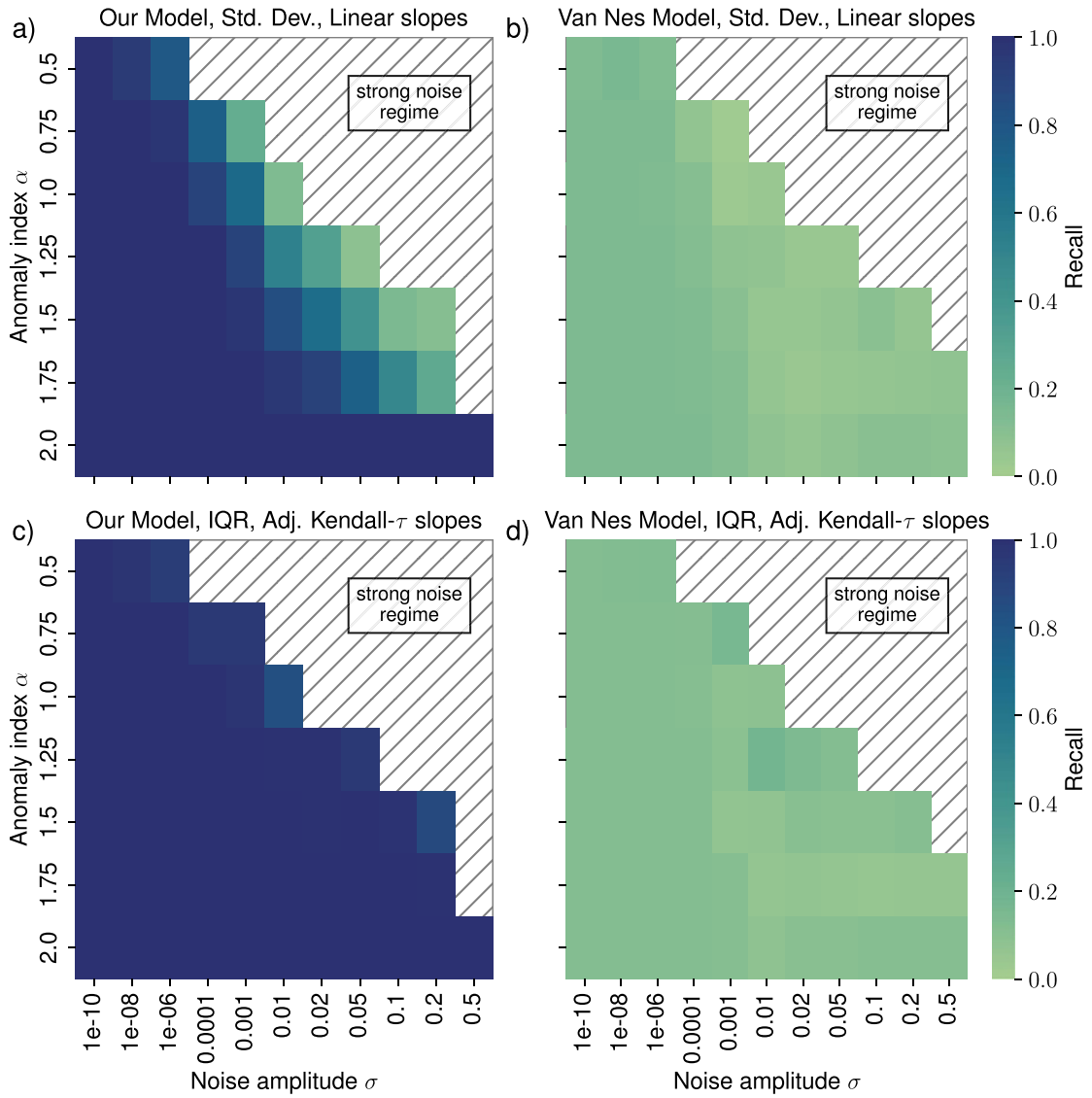

Figure 3. Recall across various noise amplitudes and anomaly indices ($\alpha = 2$ is Gaussian noise). Shown are only those noise configurations that can be considered as weak noise determined by the observed first passage time. Panels (a) & (c) show processing chains that leads to high recall, i.e. the power-law disturbances are properly dealt with. Panel (c) is slightly preferred, as recall is close to 1.0 for all noise configurations, with slight decrease close to the strong noise regime. Panels (b) & (d) in contrast show no proper treatment of power-law disturbances, which leads to low recall close to $10\% \pm 2\%$. Notably, the recall is also low for Gaussian noise ($\alpha = 2$), because the internal time scale ($\mathcal{O}(100)$ model years) in the van Nes *et al* [45] model is too long in comparison to the modeled critical transition (500 model years) to observe CSD. Thus, the van Nes *et al* [45] model can be considered unsuitable for the study of CSD indicators due to a lacking representation of short timescales.

If CSD is assessed on a filtered time series, we find a low FPR of on average 0.02 for the non-parametric Kendall-τ slope on IQR time series (figure 4(a)). Here, the filtering is leveraged as a post-hoc adjustment to assess the significance of a decline: by random chance, one might detect a significant slope even if the magnitude of the autocorrelation is very low. Hence, we flag those early warnings, where the temporal autocorrelation is below 0.5. We refer to the resulting indicator as *Adjusted Kendall-Tau Slope*. Note that the autocorrelation is particularly suitable to perform this filtering because there is a natural way of thresholding, in contrast to the standard deviation or the IQR. When including such filtering, the early warning (forest resilience) pipeline produces few false alarms.

In contrast, when early warning is detected on raw (unfiltered) time series, we detect a non-neglibile average FPR of 0.10, again for the case of non-parametric Kendall-τ slope on IQR time series (figure 4(b)). Hence, the early warning pipeline without the filtering of perturbations according to their temporal autocorrelation, raises false alarms. For an ecological system, this means a declining resilience measured solely by a CSD indicator should always be double-checked, for instance against

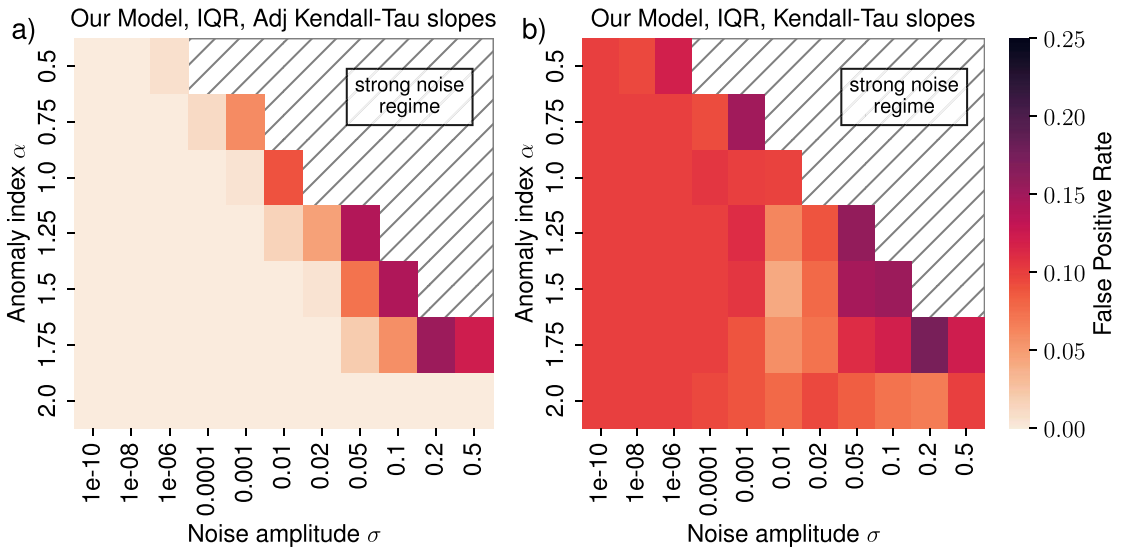

Figure 4. False positive rate (FPR) for parameter ranges also shown in figure 3. Panel (a) displays a processing chain that leads to low FPR, i.e. the power-law disturbances are properly dealt with. FPR is close to 0.0 for noise configurations far from the strong noise regime, but increases close to the strong noise regime. Panel (b) in contrast shows the effect of improper treatment of power-law disturbances. This leads to a false positive rate close to 10%, but with a higher variation across noise configurations.

Table 1. Average recall and false positive rate (FPR) for various processing chains (bold: best number per metric). Averages are computed across a wide choice of noise amplitudes and anomaly indices, as long as the resulting noise can be considered weak (as measured by the first passage time). Each row shows the result for one processing scenario for both, the original van Nes *et al* [45] model, for which CSD does not work due to a lack of representation of short timescales and for our model modification, which includes small timescale. The first block of rows presents different choices for computing the slope of the early warning indicator, here the non-linear parametric Kendall-τ slope is robust and thus preferrential. The robustness becomes clear in the second block, there is little variation in recall when comparing other early warning indicators than the interquartile-range (IQR). The final row shows that adjusting the early warning based on the absolute autocorrelation reduces the FPR by a factor of five, while keeping a high recall. In all cases, the van Nes *et al* [45] model has low Recall, which does not mean it is a bad model, simply that it is unsuitable for studying CSD indicators. Our Model modification, in turn, enables the study of CSD indicators across all processing scenarios.

		van Nes		Our Model	
Slope	Indicator	Recall	FPR	Recall	FPR
Linear	IQR	0.10	0.07	0.85	0.10
Theil-Sen	IQR	0.04	0.04	0.51	0.08
Kendall-τ	IQR	0.11	0.08	**0.99**	0.10
Kendall-τ	Std. Dev.	0.10	0.10	0.97	0.10
Kendall-τ	Lag-1 AC	0.10	0.11	0.96	0.11
Adj. Kendall-τ	IQR	0.11	0.08	**0.99**	**0.02**

the magnitude of the temporal autocorrelation in historical time series. Otherwise, a false alarm may be raised.

Table 1 summarizes the key findings by comparing mean recall and mean FPRs across a selection of scenarios. First, using Kendall-Tau slopes in our model (including short timescales), high recall can be achieved (third row). Second, adjusting the early warning for the magnitude of the autocorrelation, low false-positive rates at high recall are possible (last row). For the original van Nes *et al* [45] model, recall is always low, irrespective of the processing (third column). For our model, only the Kendall-Tau slope gives consistently high recall, linear and Theil–Sen slopes suffer from jumps in the noise structure (fifth column). The type of indicator used to assess CSD (i.e. rainforest resilience) is less relevant, we find the IQR slightly outperforms standard deviation and autocorrelation, but all three measures are valid options (rows 3–5). The average FPR before adjusting is around 10%, and can be reduced to only 2% by removing false positives with low autocorrelation.

4. Discussion

Our work suggests that CSD can be used to assess resilience loss due to an approaching critical transition also in the presence of extreme events modelled by α-stable Lévy noise. In the case of the Amazon rainforest, this confirms the empirical results by other studies indicating a destabilization of the

system [5, 7, 8, 65, 66] as being more generally applicable than previously thought.

The particular tropical rainforest model used in this study is a strongly simplified rainforest model. However, it can be understood as a special case of a very general model: a double-well potential, the mathematical normal form of a saddle-node bifurcation. For transitions in a double-well potential, our findings hold and are robust (see appendix A). Hence, they are not limited to just the particular choice of the conceptual model in this study but are more widely applicable to any system exhibiting such critical transitions. For instance, many tipping elements of the Earth system have been modelled through special cases of the double-well potential [4, 67, 68]. Also some other models of tropical rainforests [46, 69] belong to the double-well potential family. Furthermore, we claim our analysis is relevant for the actual rainforest system, which is highly complex. To support such statement, one may consider increasing complexity of the model, e.g. by studying global dynamical vegetation models. Due to their high-dimensionality, they usually cannot be easily represented by a potential landscape. However, for Coupled Model Intercomparison Project 6 models, abrupt local forest dieback has been diagnosed in the Amazon basin [70]. Hence, the existence of critical transitions is indicated and locally such a transition can again be reasonably well approximated by simple double-well potential models, as done in this study.

A similar line of thought can be employed regarding the inclusion of short timescales in the van Nes *et al* [45] rainforest model. In this study, an additional Gaussian potential was added to the rainforest stable state, implementing a fast response of the forest to small fluctuations due to weather. This modification does not alter the model globally: the stable states remain the same, only with locally varying recovery rates. A process-based implementation of the fast response rate would have a similar behavior, when coarse-grained, hence it would have similar behavor and would not qualitatively change the outcome of this study. Still, future work may consider extending the van Nes *et al* [45] model not just conceptually (as done in this study), but rather through mathematical descriptions of ecological mechanisms modulating the forests behavior on short timescales.

Not all non-Gaussian disturbances necessarily are of α-stable Lévy-type. Instead, in some circumstances, coloured noise has been observed in ecological systems and in particular in tropical rainforest [71–75]. In such cases, the two most commonly postulated colour noises are pink noise and red noise. For red noise, which displays an auto-correlated noise structure, resilience measures based on CSD indicators need to be adapted, but then they work as in the case of white noise [37]. Pink noise has power-law tails but does not lead to jumps in the forest state evolution. Therefore, we find that our results for α-stable Lévy noise are robust for pink noise (see appendix B and table B1 for details). Hence, for a wide range of non-Gaussian noise observed in ecology, CSD indicators are valid choices to measure tropical rainforest resilience.

Two further points regarding the accuracy of our mathematical model require caution: first, we have chosen to model forest disturbances via α-stable Lévy noise to honour the prevalence of extreme events in observations. However, as the variable representing the state of the rainforest is bounded between 0 and 100% (tree cover density), the far end of the noise tail needs to be disregarded, because tree cover cannot fall below 0% nor go beyond 100%. This restricts the conceptual modelling capabilities of the α-stable noise model. It does however not pose a practical problem for interpreting the model data as observations from a multi-stable forest system because an exceedingly extreme disturbance always simply leads to a tipped system. Our work demonstrates that the concept of CSD holds in the case of α-stable noise distributions when observing the time span before tipping. Second, due to ongoing deforestation for many decades, one might argue the Amazon is not in a steady state, but rather on a transient. Hence, the equilibrium assumption of CSD, whereby a slow change in the external forcing only changes the equilibrium state, but does not keep the system in disequilibrium for long, may be violated. Nevertheless, studies have found that the Amazon rainforest may approach a tipping point due to deforestation [76, 77].

5. Conclusion

We find robustness of CSD indicators used to measure resilience in multi-stable systems driven by α-stable Lévy noise. The presence of disturbances with power-law spectrum occurring in single discrete jumps does not affect the identification of early warning of a critical transition as long as the jump size is small enough to avoid immediate, noise-induced transitions between alternative stable states. For this purpose, we find it is ideal to test the IQR with Kendall-Tau slope for significant increases and filter for cases with low autocorrelation. With such processing, high recall and low FPRs can be achieved. Most recent work computing resilience indicators based on remote sensing in the Amazon basin follow a similar procedure [7, 30]. In particular, they assess rainforest resilience with CSD indicators and find a resilience decline. Our work emphasizes that such empirical findings are not corroborated in the presence of non-Gaussian disturbances, which could not be ruled out

previously. Hence, it adds to the increasing evidence that the Amazon rainforest's resilience has been declining in recent decades, irrespective of the actual nature of the noise (white, coloured, or Lévy noise). Future work may proceed in two manners. First, it may extend the analysis to include a spatial component. Spatial processes are highly relevant for tropical vegetation health and resulting spatial patterns [43, 44], e.g. patchiness, have been introduced as another type of early warning signal (i.e. resilience indicator) [78]. Second, it may study the effectiveness of different noise types in simulating remotely sensed rainforest health indices, for instance through estimating the exact power law in different vegetation health indicators with statistical tests.

Data availability statement

The data that support the findings of this study are openly available at the following URL/DOI: http://doi.org/10.5281/zenodo.10001350 [79].

Acknowledgments

N W and J F D acknowledge support from the European Research Council Advanced Grant project ERA (Earth Resilience in the Anthropocene, ERC-2016-ADG-743080). J F D is grateful for financial support by the German Federal Ministry for Education and Research (BMBF) (project 'PIK Change', grant 01LS2001A). N B acknowledges funding by the Volkswagen foundation and by the European Union's Horizon 2020 research and innovation programme under the Marie Sklodowska-Curie Grant Agreement No. 956170, and under Grant Agreement No. 820970. A S was supported by the Dutch Research Council (NWO) Talent Program Grant VI.Veni.202.170. M H thanks the Serrapilheira Institute (Grant Number Serra-1709-18983).

Code to reproduce results

https://github.com/vitusbenson/tropical_rainforest_resilience_nongaussian

Appendix A. Double-well potential

We repeat our α-stable Lévy noise experiments with a generic model based on a double-well potential. More specifically, we construct a double-well potential with similar timescales and value range as the Amazon model with short timescales introduced in the main body of this work. Let $x \in [0, 100]$ be an abstraction of the rainforest state and $c \in \mathbb{R}$ be an external forcing (think *climate change*). Our model becomes the first-order ODE:

$$\frac{\mathrm{d}x}{\mathrm{d}t} = \frac{\tau}{a}\left(\left(\frac{x}{a}+b\right)^3 + \frac{x}{a} + b - \frac{4\sqrt{4}}{27}c\right) + \mathrm{d}N_t. \tag{A.1}$$

With a timescale $\tau = 1000$, a value range $a = 20$ and a value shift $b = -3$ as fixed parameters. For $c < -1$, equation (A.1) has one stable fixed point (the rainforest state, $x \approx 80$), for $-1 \leqslant c \leqslant 1$, there are two stable fixed points exist and for $c > 1$ there is again only one stable fixed point exists (the savannah state $x \approx 40$). As in the main text, we choose α-stable Lévy noise for the noise term $\mathrm{d}N_t$.

These parameter settings allow us to perform simulations in the same set-up as described in figure 1, with the minor difference that we simulate climate change by linearly increasing the forcing from $c = -1.5$ to $c = 1.5$. The results are consistent with those in the main body. Figure A1 shows the recall across a variety of noise settings, for two cases: 1. adjusted Kendall-Tau slopes on the IQR, where recall is always high, and 2. linear slopes on the standard deviation, where some deterioration in recall can be observed towards the strong noise regime. The adjustment for a low FPR is less effective in the case of the double-well potential: without it, Kendall-Tau slopes on IQR get 9.3% false positives, while with the adjustment, the FPR drops to 8.6%. Likely this is due to the threshold of $AC(1) = 0.5$ introduced in the main body, which seems valid for the Amazon rainforest model, but not for the double-well potential.

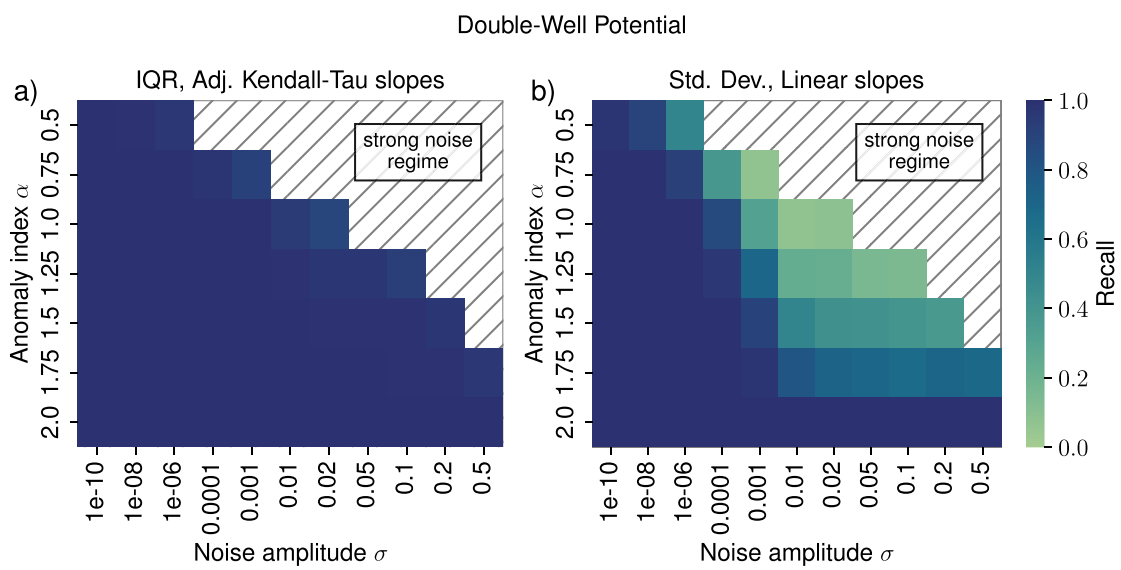

Figure A1. Same as figures 3(c) and (b), but using a double-well potential as the model. Recall across various noise amplitudes and anomaly indices ($\alpha = 2$ is Gaussian noise). Shown are only those noise configurations that can be considered as weak noise determined by the observed first passage time. Panel (a) shows a processing chain that leads to high recall, i.e. the power-law disturbances are properly dealt with. Recall is close to 1.0 for all noise configurations, with a slight decrease close to the strong noise regime. Panel (b) in contrast shows no proper treatment of power-law disturbances, which leads to reduced recall closer to the strong noise regime.

Table B1. Same as table 1, but for pink noise. Recall and false positive rate (FPR) for various processing chains (bold: best number per metric). Averages are computed across a wide choice of noise amplitudes, as long as the resulting noise can be considered weak (as measured by the first passage time). The columns 3–4 show results for the original van Nes *et al* [45] model, for which critical slowing down does not work due to a lack of representation of short timescales. Columns 5–6 our model, which includes short timescales. The third row shows the non-linear Kendall-Tau slope is robust and thus preferrential. The robustness becomes clear in rows 3–5, there is little variation in recall when comparing other early warning indicators than the interquartile-range (IQR). The final row shows that adjusting the early warning based on the absolute temporal autocorrelation reduces the FPR to zero, while keeping a high recall. In all cases, the van Nes *et al* [45] model has low Recall, which does not mean it is a bad model, simply that it is unsuitable for studying CSD indicators. Our Model modification, in turn, enables the study of CSD indicators across all processing scenarios.

		van Nes		Our Model	
Slope	Indicator	Recall	FPR	Recall	FPR
Linear	IQR	0.16	0.08	0.98	0.12
Theil-Sen	IQR	0.04	0.04	0.36	0.09
Kendall-τ	IQR	0.12	0.08	**0.99**	0.11
Kendall-τ	Std. Dev.	0.14	0.09	0.99	0.11
Kendall-τ	Lag-1 AC	0.19	0.11	0.99	0.09
Adj. Kendall-τ	IQR	0.12	0.08	**0.99**	**0.00**

Appendix B. Pink noise

We generate pink noise by first generating Gaussian noise, taking its Fourier transform, dividing each amplitude by the square root of its frequency and then transforming inversely. We then perform simulations for a range of noise amplitudes using the same Amazon rainforest models described in section 2 (both, the van Nes *et al* [45] original, and our variation including short timescales). We enforce negative disturbances by mirroring the pink noise at the origin, but we keep a small additional Gaussian noise term to represent climatic variations.

The results are presented in table B1 and are consistent with the α-stable Lévy noise results. A high recall and a low FPR can be achieved by using adjusted Kendall-tau slopes on the IQR in our model (which includes short timescales).

Appendix C. Linear Langevin dynamics under α-stable noise forcing

We have relayed the motivation behind employing variance and AC(1) as indicators for changes in system stability in the main text. This theoretical treatment regarded a linearised model under white noise forcing (see equation (6)). The analytical quantities of variance and AC(1) in equations (7) and (8) directly arise from this model and approximate the expected quantities in applications to real bifurcation dynamics. The restoring rate λ is a metric for system stability and vanishes when crossing a co-dimension

1 bifurcation. Insofar as a natural system can be viewed as being in equilibrium and experiencing small Gaussian white noise disturbances, the derived expressions dictate an increase in variance and AC(1) as the system approaches a critical transition. In the present work, we propose that Gaussian white noise forcing is an inadequate modelling choice for e.g. forest dynamics, as extreme disturbances are regularly observed. The question of whether the equilibrium dynamics of a linearised system under asymmetric, heavy-tailed noise forcing allows for a similar technique to assess CSD points to the following Langevin equation,

$$\mathrm{d}x_t = \lambda\left(x_t - x^*\right)\mathrm{d}t + \sigma \mathrm{d}L_t^{\alpha}, \tag{C.1}$$

where we assume here w.l.o.g. that $x^* = 0$. As in the main text, the noise term $\sigma \mathrm{d}L_t^{\alpha}$ is assumed to be α-stable Levy-noise with $\alpha < 1$, skewness parameter $\beta = -1$, and scaling parameter $c = \sigma \mathrm{d}t^{1/\alpha}$. The increments $\sigma \mathrm{d}L_t^{\alpha}$ are independent of each other. Their characteristic function is given by

$$\begin{aligned}\phi_{\sigma \mathrm{d}L^{\alpha}}(s) &= \exp\left(is\mu - |cs|^{\alpha}\left(1 - i\beta \mathrm{sgn}(s)\tan(\pi\alpha/2)\right)\right)\\ &= \exp\left(-|\sigma \mathrm{d}t^{1/\alpha}s|^{\alpha}\left(1 + i\,\mathrm{sgn}(s)\tan(\pi\alpha/2)\right)\right).\end{aligned}$$

We will first show that there exists a stationary solution to equation (C.1), which is itself α-stable. We can write the Euler–Mayurama discretisation corresponding to equation (C.1) as

$$\begin{aligned}x_{t+\Delta t}^{(\Delta t)} - x_t^{(\Delta t)} &= \lambda x_t^{(\Delta t)}\Delta t + \sigma \Delta L_t^{\alpha}\\ \Leftrightarrow x_{t+\Delta t}^{(\Delta t)} &= (1 + \lambda\Delta t)\, x_t^{(\Delta t)} + \sigma \Delta L_t^{\alpha}.\end{aligned} \tag{C.2}$$

In the limit of $\Delta t \to 0$, this autoregressive process converges to a solution of the continuous-time Langevin equation (C.1). Ansatz: assume that $x^{(\Delta t)}$ is itself $\alpha_{x^{(\Delta t)}}$-stable with parameters $\beta_{x^{(\Delta t)}}$ and $c_{x^{(\Delta t)}}$. For this to be a stationary distribution, one can see via induction on the discrete-time equation that first two the parameters must be the same as those of the noise, i.e. $\alpha_{x^{(\Delta t)}} = \alpha$ and $\beta_{x^{(\Delta t)}} = \beta = -1$. The correct choice of $c_{x^{(\Delta t)}}$ remains to be calculated. For this, notice that the two random variables on the right-hand side of equation (C.2) are independent, so the characteristic function of the total must be the product of the two individual ones:

$$\begin{aligned}&\phi_{x^{(\Delta t)}}(s) = \phi_{(1+\lambda\Delta t)x^{(\Delta t)}}(s)\,\phi_{\sigma\Delta L^{\alpha}}(s)\\ &\Leftrightarrow \exp\left(\left(-|c_{x^{(\Delta t)}}s|^{\alpha}\left(1 + i\,\mathrm{sgn}(s)\tan(\pi\alpha/2)\right)\right)\right)\\ &= \exp\left(-\left(\left|(1+\lambda\Delta t)\, c_{x^{(\Delta t)}}s\right|^{\alpha} + |\sigma\Delta t^{1/\alpha}s|^{\alpha}\right)\right.\\ &\quad\left.\times\left(1 + i\,\mathrm{sgn}(s)\tan(\pi\alpha/2)\right)\right)\\ &\Leftrightarrow |c_{x^{(\Delta t)}}s|^{\alpha} = \left|(1+\lambda\Delta t)\, c_{x^{(\Delta t)}}s\right|^{\alpha} + |\sigma\Delta t^{1/\alpha}s|^{\alpha}\\ &\Leftrightarrow c_{x^{(\Delta t)}}^{\alpha} = (1+\lambda\Delta t)^{\alpha}\, c_{x^{(\Delta t)}}^{\alpha} + \sigma^{\alpha}\Delta t\\ &\Leftrightarrow c_{x^{(\Delta t)}}^{\alpha} = \frac{\sigma^{\alpha}\Delta t}{1 - (1+\lambda\Delta t)^{\alpha}}.\end{aligned}$$

In the limit of $\Delta t \to 0$, this implies that

$$c_x^{\alpha} = \frac{-\sigma^{\alpha}}{\alpha\lambda}.$$

This result is consistent with the known variance $c_x^2 = \frac{-\sigma^2}{2\lambda}$ for the Gaussian white noise case of $\alpha = 2$.

Since the scaling parameter c_x dictates the distribution width of the observed process, we may posit a direct influence of the linear restoring rate λ on the observed variance and the IQR, analogous to the case of Gaussian white noise. We have to bear in mind however, that in this setting of an unbounded observable, the variance of the α-stable distribution is ill-defined and will numerically diverge to infinity when applying law of large numbers estimators. In the application of a bounded forest state variable, we expect the finite variance to be an increasing function of λ, which can thus function as a CSD indicator. Further analysis is needed to theoretically motivate the use of AC(1) in a similar fashion. However, as has been laid out during the analysis within the main text, its use is warranted on a numerical basis.

ORCID iDs

Vitus Benson https://orcid.org/0000-0003-4760-5501
Jonathan F Donges https://orcid.org/0000-0001-5233-7703
Niklas Boers https://orcid.org/0000-0002-1239-9034
Marina Hirota https://orcid.org/0000-0002-1958-3651
Andreas Morr https://orcid.org/0000-0002-9804-5180
Arie Staal https://orcid.org/0000-0001-5409-1436
Jürgen Vollmer https://orcid.org/0000-0002-8135-1544
Nico Wunderling https://orcid.org/0000-0002-3566-323X

References

[1] Mitchard E T A 2018 The tropical forest carbon cycle and climate change *Nature* **559** 527–34
[2] Armstrong McKay D I, Staal A, Abrams J F, Winkelmann R, Sakschewski B, Loriani S, Fetzer I, Cornell S E, Rockström J and Lenton T M 2022 Exceeding 1.5 °C global warming could trigger multiple climate tipping points *Science* **377** eabn7950
[3] Boers N, Ghil M and Stocker T F 2022 Theoretical and paleoclimatic evidence for abrupt transitions in the Earth system *Environ. Res. Lett.* **17** 093006
[4] Lenton T M, Held H, Kriegler E, Hall J W, Lucht W, Rahmstorf S and Schellnhuber H J 2008 Tipping elements in the Earth's climate system *Proc. Natl Acad. Sci.* **105** 1786–93
[5] Nobre C A, Sampaio G, Borma L S, Castilla-Rubio J C, Silva J S and Cardoso M 2016 Land-use and climate change risks in the Amazon and the need of a novel sustainable development paradigm *Proc. Natl Acad. Sci.* **113** 10759–68
[6] Davidson E A *et al* 2012 The Amazon basin in transition *Nature* **481** 321–8

[7] Boulton C A, Lenton T M and Boers N 2022 Pronounced loss of Amazon rainforest resilience since the early 2000s *Nat. Clim. Change* **12** 271–8
[8] Lovejoy T E and Nobre C 2018 Amazon tipping point *Sci. Adv.* **4** eaat2340
[9] Hirota M, Holmgren M, Van Nes E H and Scheffer M 2011 Global resilience of tropical forest and savanna to critical transitions *Science* **334** 232–5
[10] Staver A C, Archibald S and Levin S A 2011 The global extent and determinants of savanna and forest as alternative biome states *Science* **334** 230–2
[11] Ciemer C, Boers N, Hirota M, Kurths J, Müller-Hansen F, Oliveira R S and Winkelmann R 2019 Higher resilience to climatic disturbances in tropical vegetation exposed to more variable rainfall *Nat. Geosci.* **12** 174–9
[12] Staal A, Fetzer I, Wang-Erlandsson L, Bosmans J H C, Dekker S C, van Nes E H, Rockström J and Tuinenburg O 2020 A Hysteresis of tropical forests in the 21st century *Nat. Commun.* **11** 4978
[13] Wunderling N, Staal A, Sakschewski B, Hirota M, Tuinenburg O A, Donges J F, Barbosa H M J and Winkelmann R 2022 Recurrent droughts increase risk of cascading tipping events by outpacing adaptive capacities in the Amazon rainforest *Proc. Natl Acad. Sci.* **119** e2120777119
[14] Saatchi S *et al* 2021 Detecting vulnerability of humid tropical forests to multiple stressors *One Earth* **4** 988–1003
[15] Bastos A, Sippel S, Frank D, Mahecha M D, Zaehle S, Zscheischler J and Reichstein M 2023 A joint framework for studying compound ecoclimatic events *Nat. Rev. Earth Environ.* **4** 333–50
[16] Fisher J I, Hurtt G C, Thomas R Q and Chambers J Q 2008 Clustered disturbances lead to bias in large-scale estimates based on forest sample plots *Ecol. Lett.* **11** 554–63
[17] Taubert F, Fischer R, Groeneveld J, Lehmann S, Müller M S, Rödig E, Wiegand T and Huth A 2018 Global patterns of tropical forest fragmentation *Nature* **554** 519–22
[18] Gloor M *et al* 2009 Does the disturbance hypothesis explain the biomass increase in basin-wide Amazon forest plot data? *Glob. Change Biol.* **15** 2418–30
[19] Espírito-Santo F D B, Keller M, Braswell B, Nelson B W, Frolking S and Vicente G 2010 Storm intensity and old-growth forest disturbances in the Amazon region *Geophys. Res. Lett.* **37** 11
[20] Negrón-Juárez R I, Chambers J Q, Guimaraes G, Zeng H, Raupp C F M, Marra D M, Ribeiro G H P M, Saatchi S S, Nelson B W and Higuchi N 2010 Widespread Amazon forest tree mortality from a single cross-basin squall line event *Geophys. Res. Lett.* **37** 16
[21] Asner G P, Kellner J R, Kennedy-Bowdoin T, Knapp D E, Anderson C and Martin R E 2013 Forest canopy gap distributions in the Southern Peruvian Amazon *PLoS One* **8** e60875
[22] Chambers J Q, Negron-Juarez R I, Marra D M, Di Vittorio A, Tews J, Roberts D, Ribeiro G H P M, Trumbore S E and Higuchi N 2013 The steady-state mosaic of disturbance and succession across an old-growth Central Amazon forest landscape *Proc. Natl Acad. Sci.* **110** 3949–54
[23] Espírito-Santo F D B *et al* 2014 Size and frequency of natural forest disturbances and the Amazon forest carbon balance *Nat. Commun.* **5** 3434
[24] Reis C R, Jackson T D, Gorgens E B, Dalagnol R, Jucker T, Nunes M H, Ometto J P, Aragão L E O C, Rodriguez L C E and Coomes D A 2022 Forest disturbance and growth processes are reflected in the geographical distribution of large canopy gaps across the Brazilian Amazon *J. Ecol.* **110** 2971–83
[25] Stocker B D, Zscheischler J, Keenan T F, Prentice I C, Seneviratne S I and Pe ñuelas J 2019 Drought impacts on terrestrial primary production underestimated by satellite monitoring *Nat. Geosci.* **12** 264–70
[26] Zscheischler J, Mahecha M D, Harmeling S and Reichstein M 2013 Detection and attribution of large spatiotemporal extreme events in Earth observation data *Ecol. Inf.* **15** 66–73
[27] Reichstein M *et al* 2013 Climate extremes and the carbon cycle *Nature* **500** 287–95
[28] Cano-Crespo A, Traxl D, Prat-Ortega G, Rolinski S and Thonicke K 2022 Characterization of land cover-specific fire regimes in the Brazilian Amazon *Reg. Environ. Change* **23** 19
[29] Nicoletti G, Saravia L, Momo F, Maritan A and Suweis S 2023 The emergence of scale-free fires in Australia *iScience* **26** 106181
[30] Smith T, Traxl D and Boers N 2022 Empirical evidence for recent global shifts in vegetation resilience *Nat. Clim. Change* **12** 1–8
[31] Lenton T M, Buxton J E, Armstrong McKay D I, Abrams J F, Boulton C A, Lees K, Powell T W R, Boers N, Cunliffe A M and Dakos V A 2022 Resilience sensing system for the biosphere *Phil. Trans. R. Soc.* B **377** 20210383
[32] Forzieri G, Dakos V, McDowell N G, Ramdane A and Cescatti A 2022 Emerging signals of declining forest resilience under climate change *Nature* **608** 534–9
[33] Liu Y, Kumar M, Katul G G and Porporato A 2019 Reduced resilience as an early warning signal of forest mortality *Nat. Clim. Change* **9** 880–5
[34] Krakovská H, Kuehn C and Longo I P 2023 Resilience of dynamical systems *Eur. J. Appl. Math.* **35** 1–46
[35] van Nes E H and Scheffer M 2007 Slow recovery from perturbations as a generic indicator of a nearby catastrophic shift *Am. Nat.* **169** 738–47
[36] Boettner C and Boers N 2022 Critical slowing down in dynamical systems driven by nonstationary correlated noise *Phys. Rev. Res.* **4** 013230
[37] Morr A and Boers N 2023 Detection of approaching critical transitions in natural systems driven by red noise (arXiv:2310.05587)
[38] Gnedenko B V and Kolmogorov A N 1954 *Limit Distributions for Sums of Independent Random Variables* (Addison-Wesley Pub. Co.)
[39] Embrechts P, Klüppelberg C and Mikosch T 1997 *Modelling Extremal Events* (Springer)
[40] Ditlevsen P D 1999 Anomalous jumping in a double-well potential *Phys. Rev.* E **60** 172–9
[41] Serdukova L, Zheng Y, Duan J and Kurths J 2017 Metastability for discontinuous dynamical systems under Lévy noise: case study on Amazonian Vegetation *Sci. Rep.* **7** 9336
[42] Dutta P S, Sharma Y and Abbott K C 2018 Robustness of early warning signals for catastrophic and non-catastrophic transitions *Oikos* **127** 1251–63
[43] Bastiaansen R, Doelman A, Eppinga M B and Rietkerk M 2020 The effect of climate change on the resilience of ecosystems with adaptive spatial pattern formation *Ecol. Lett.* **23** 414–29
[44] Rietkerk M, Bastiaansen R, Banerjee S, van de Koppel J, Baudena M and Doelman A 2021 Evasion of tipping in complex systems through spatial pattern formation *Science* **374** eabj0359
[45] van Nes E H, Hirota M, Holmgren M and Scheffer M 2014 Tipping points in tropical tree cover: linking theory to data *Glob. Change Biol.* **20** 1016–21
[46] Staal A, Dekker S C, Hirota M and van Nes E H 2015 Synergistic effects of drought and deforestation on the resilience of the south-eastern Amazon rainforest *Ecol. Complexity* **22** 65–75
[47] Martinez-Ramos M, Alvarez-Buylla E, Sarukhan J and Pinero D 1988 Treefall age determination and gap dynamics in a tropical forest *J. Ecol.* **76** 700–16
[48] Vicente-Serrano S M *et al* 2013 Response of vegetation to drought time-scales across global land biomes *Proc. Natl Acad. Sci.* **110** 52–57
[49] Linscheid N, Estupinan-Suarez L M, Brenning A, Carvalhais N, Cremer F, Gans F, Rammig A, Reichstein M, Sierra C A and Mahecha M D 2020 Towards a global

understanding of vegetation- climate dynamics at multiple timescales *Biogeosciences* **17** 945–62
[50] Sierra C A, Estupinan-Suarez L M and Chanca I 2021 The fate and transit time of carbon in a tropical forest *J. Ecol.* **109** 2845–55
[51] Feldpausch T R *et al* 2016 Amazon forest response to repeated droughts *Glob. Biogeochem. Cycles* **30** 964–82
[52] Esquivel-Muelbert A *et al* 2019 Compositional response of Amazon forests to climate change *Glob. Change Biol.* **25** 39–56
[53] Meir P, Wood T E, Galbraith D R, Brando P M, Da Costa A C L, Rowland L and Ferreira L V 2015 Threshold responses to soil moisture deficit by trees and soil in tropical rain forests: insights from field experiments *BioScience* **65** 882–92
[54] Rowland L *et al* 2015 Death from drought in tropical forests is triggered by hydraulics not carbon starvation *Nature* **528** 119–22
[55] Doughty C E *et al* 2023 Tropical forests are approaching critical temperature thresholds *Nature* **621** 105–11
[56] Farrior C E, Bohlman S A, Hubbell S and Pacala S W 2016 Dominance of the suppressed: power-law size structure in tropical forests *Science* **351** 155–7
[57] Negrón-Juárez R I *et al* 2018 Vulnerability of Amazon forests to storm-driven tree mortality *Environ. Res. Lett.* **13** 054021
[58] Lévy P 1924 Théorie des erreurs. La loi de Gauss et les lois exceptionnelles *Bull. Soc. Mat. Fr.* **2** 49–85
[59] Chechkin A V, Metzler R, Klafter J and Gonchar V Y 2008 Introduction to the theory of Lévy flights *Anomalous Transport* ed R Klages, G Radons and I M Sokolov (Wiley-VCH Verlag GmbH & Co. KGaA) pp 129–62
[60] Janicki A and Weron A 1994 *Simulation and Chaotic Behavior of [Alpha]-Stable Stochastic Processes* (*Monographs and Textbooks in Pure and Applied Mathematics*) (M. Dekker)
[61] Wissel C A 1984 universal law of the characteristic return time near thresholds *Oecologia* **65** 101–7
[62] Dakos V, Scheffer M, van Nes E H, Brovkin V, Petoukhov V and Held H 2008 Slowing down as an early warning signal for abrupt climate change *Proc. Natl Acad. Sci.* **105** 5
[63] Scheffer M, Bascompte J, Brock W A, Brovkin V, Carpenter S R, Dakos V, Held H, van Nes E H, Rietkerk M and Sugihara G 2009 Early-warning signals for critical transitions *Nature* **461** 53–59
[64] Boers N 2021 Observation-based early-warning signals for a collapse of the Atlantic meridional overturning circulation *Nat. Clim. Change* **11** 680–8
[65] Lovejoy T E and Nobre C 2019 Amazon tipping point: last chance for action *Sci. Adv.* **5** eaba2949
[66] Flores B M and Holmgren M 2021 White-sand savannas expand at the core of the Amazon after forest wildfires *Ecosystems* **24** 1624–37
[67] Wunderling N, Donges J F, Kurths J and Winkelmann R 2021 Interacting tipping elements increase risk of climate domino effects under global warming *Earth Syst. Dyn.* **12** 601–19
[68] Wunderling N, Winkelmann R, Rockström J, Loriani S, Armstrong McKay D I, Ritchie P D L, Sakschewski B and Donges J F 2023 Global warming overshoots increase risks of climate tipping cascades in a network model *Nat. Clim. Change* **13** 75–82
[69] Da Silveira Lobo Sternberg L 2001 Savanna-forest hysteresis in the tropics *Glob. Ecol. Biogeogr.* **10** 369–78
[70] Parry I M, Ritchie P D L and Cox P M 2022 Evidence of localised Amazon rainforest dieback in CMIP6 models *Earth Syst. Dyn.* **13** 1667–75
[71] Halley J M 1996 Ecology, evolution and 1f-noise *Trends Ecol. Evol.* **11** 33–37
[72] Halley J M and Inchausti P 2004 The increasing importance of 1f-noises as models of ecological variability *Fluct. Noise Lett.* **04** R1–R26
[73] Newbery D M, Lingenfelder M, Poltz K F, Ong R C and Ridsdale C E 2011 Growth responses of understorey trees to drought perturbation in tropical rainforest in Borneo *Forest Ecol. Manage.* **262** 2095–107
[74] Vasseur D A and Yodzis P 2004 The color of environmental noise *Ecology* **85** 1146–52
[75] Yang Q, Fowler M S, Jackson A L and Donohue I 2019 The predictability of ecological stability in a noisy world *Nat. Ecol. Evol.* **3** 251–9
[76] Boers N, Marwan N, Barbosa H M J and Kurths J 2017 A deforestation-induced tipping point for the South American monsoon system *Sci. Rep.* **7** 41489
[77] Bochow N and Boers N 2023 The South American monsoon approaches a critical transition in response to deforestation *Sci. Adv.* **9** eadd9973
[78] Dakos V, van Nes E H, Donangelo R, Fort H and Scheffer M 2010 Spatial correlation as leading indicator of catastrophic shifts *Theor. Ecol.* **3** 163–74
[79] Benson V 2023 Simulation output for manuscript measuring tropical rainforest resilience under non-Gaussian disturbances *Zenodo* (https://doi.org/10.5281/zenodo.10001351)